UNIVERSITY
of
GLASGOW

Sheng, W. and Galbraith, R. A. McD. and Coton, F. N. (2006) A new stall onset criterion for low speed dynamic stall. *Journal of Solar Energy Engineering* 128(4):pp. 461-471.

http://eprints.gla.ac.uk/3381/

Glasgow ePrints Service
http://eprints.gla.ac.uk

A New Stall-Onset Criterion for Low Speed Dynamic-Stall

W. Sheng

Research Assistant

Department of Aerospace Engineering

University of Glasgow

Glasgow, G12 8QQ, UK

Email: wsheng@aero.gla.ac.uk

R. A. McD. Galbraith

Professor

Department of Aerospace Engineering

University of Glasgow

Glasgow, G12 8QQ, UK

e-mail: roddy@aero.gla.ac.uk

F. N. Coton

Professor

Department of Aerospace Engineering

University of Glasgow

Glasgow, G12 8QQ, UK

e-mail: frank@aero.gla.ac.uk

Abstract: *The Beddoes/Leishman dynamic-stall model has become one of the most popular for the provision of unsteady aerofoil data embedded in much larger codes. The underlying modelling philosophy was that it should be based on the best understanding, or description, of the associated physical phenomena. Even although the model was guided by the flow physics, it requires significant empirical inputs in the form of measured coefficients and constants. Beddoes provided these for a Mach number range of 0.3 to 0.8. This paper considers one such input for a Mach number of 0.12, where, from the Glasgow data, it is shown that the current stall-onset criterion, and subsequent adjustments, yield problematic results. A new stall criterion is proposed and developed in the best traditions of the model. It is shown to be very capable of reconstructing the Glasgow's data for stall onset both the ramp-up and oscillatory tests.*

Keywords: unsteady aerodynamics, dynamic stall, onset of dynamic stall

1 Introduction

Dynamic stall is a term used to describe the stalling of an aerofoil, or lifting surface, during unsteady flow conditions. These conditions are normally associated with pitching and plunging motions and were initially of much interest to helicopter rotor-aerodynamicists, who required an assessment of rotor loads during forward and manoeuvring flight. Today, dynamic stall is also relevant to the performance and durability of wind turbines.

Carr [4] gives an illustration for the events of a dynamic stall process, for an aerofoil undergoing a sinusoidal pitch profile, shown in Figure 1. Chronologically, the dynamic stall events start at point (a), where the pitching aerofoil passes the static-stall angle of attack, but without any discernible change in the flow around the airfoil, and the flow remains fully attached. Then the flow reverses near the surface at the trailing edge region starting at point (b), but still with no large separation due to the dynamic effects. This reversal moves up the chord until it covers most of the aerofoil, at which stages ((c) and (d)) the leading edge flow no longer remains attached and a strong vortical flow develops (point (e)). As the vortex enlarges and remains close to the leading edge, there is an obvious increase in the lift-curve slope at (f) and associated vortically induced normal force coefficient, C_N , ((g) and (h)). The vortex subsequently convects downstream and finally detaches from the trailing edge, inducing a strong nose-down pitching moment at (i). After that, when the flow over the aerofoil upper surface is fully separated, the lift break (lift stall) occurs (j). As the angle of attack decreases continuously, the reattachment process takes place. According to Niven et al [5], at some angle of attack (close to the static fully-stalled state), the leading edge reattachment occurs. This is characterised by two distinct but related events. First, all the large eddies, due to the stall, are convected over the chord and into the free stream at constant speed and, second, following closely behind is the re-establishment of a fully attached boundary layer. The convective component, i.e. the first, normally takes a few chord lengths of free-stream travel, at which point the lift reaches its lowest value. Then the flow transits to a fully attached state at the end of stage (k). Obviously, the whole process forms a large hysteresis loop, shown in figure 1, which is taken from Carr et al. [6].

Leishman [7] explores the flow topology of dynamic stall and summarises that the aerofoil dynamic behaviour is significantly different from the steady case in following three aspects:

- Under dynamic conditions, since the circulation is shed into the wake at the trailing edge of the aerofoil, the induced unsteadiness causes a reduction in the lift and adverse pressure gradients, compared to the steady case at the same angle of attack,
- By virtue of induced camber effects, a positive pitch rate further decreases the pressure and pressure gradients at the leading edge for a given value of lift,
- In response to the external pressure gradients, additional unsteady effects occur within the boundary layer, including the existence of flow reversals without any significant separation.

To avoid such adverse effects (i.e. dynamic stall) rotor designs were often very conservative. However, as technology has developed, these design constraints have been progressively relaxed, as on the case of the RAE series aerofoils (Wilby [8]) developed within the British Experimental Rotor Programme (BERP).

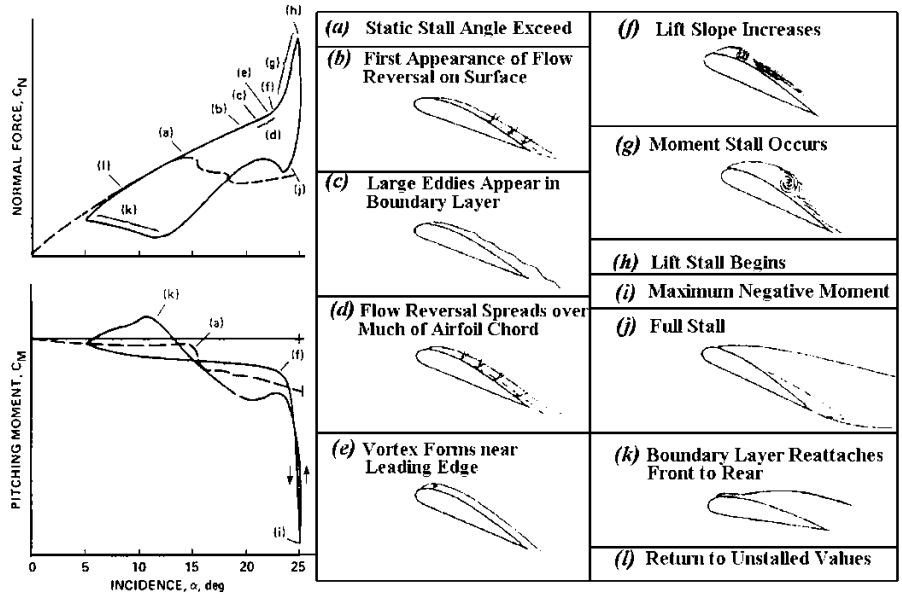

Figure 1 Events of dynamic stall process (adopted from Carr et al. [6])

During that programme, and from a series of nominally two-dimensional unsteady-aerofoil experiments, Wilby reported the existence of a critical incidence, during quarter chord pitching motions, beyond which the adverse effects of dynamic stall were unavoidable, irrespective of the aerofoil's subsequent motion. Whist this was a very important observation, since it limits the maximum pitch of a helicopters rotor for particular flight conditions, it was not, as Wilby stated, the onset of dynamic stall. In a comprehensive computer code for the prediction of helicopter or wind turbine rotor aerodynamics, the exceeding, or otherwise, of the critical angle, could only be assessed if a suitable dynamic-stall model was available. Any such model requires an appropriate stall-onset criterion.

Over the years, many models for the behaviour of aerofoils in unsteady flow conditions have been proposed [1-3], [9-13], including those based on CFD [14,15]. For the present work, the authors' have constrained their considerations to the Beddoes/Leishman model.

Beddoes original dynamic-stall model was developed in 1970s. After many refinements and improvements (Beddoes [1,16,17], Leishman & Beddoes [2,18,19]), the latest vision of Beddoes/Leishman dynamic-stall model was finalised in 1993 [3], titled the 3rd generation dynamic-stall model.

It is comprised of indicial functions for the assessment of attached flow. These are configured to permit the modelling of, for example, blade-vortex interaction. Further inclusions were the modelling unsteady trailing-edge separation, stall vortex formation and convection. The stall criteria were two fold and presented as C_{N1} against Mach number as illustrated in Figure 2.

These criteria are presented in the form of a critical normal-force coefficient. For Mach numbers greater than 0.3 a shock reversal condition is used (see Beddoes [20]) whilst for less than 0.3 a leading edge criterion, developed from the work of Evans& Mort [21] is used. The work described in the present paper considers a new criterion for low speed dynamic stall.

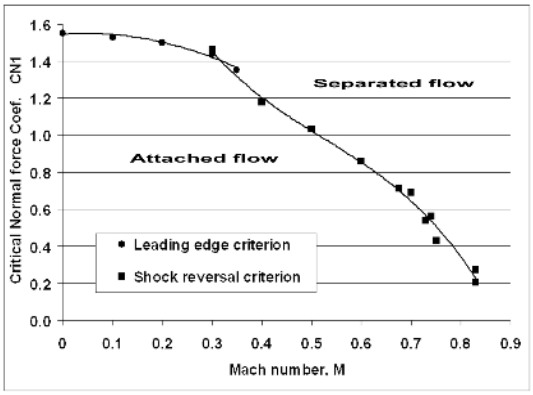

Figure 2 The Beddoes stall criteria for aerofoil NACA0012 (reproduced from Leishman et al [2])

The Evans-Mort criterion (Figure 3) was developed on the basis of static data and essentially relates the peak suction and adverse pressure gradient in the region of the leading edge at stall. Attainment of the Evans and Mort criterion corresponded to particular values of normal force and incidence for a given aerofoil. Beddoes used this critical value of C_N to indicate stall onset within his method.

Figure 3 depicts the correlation, as adopted by Niven & Galbraith [22] to include their assessment of upper and lower bounds. The Evans-Mort data, for peak velocity and ΔS_1, a measure of the adverse pressure gradient, were obtained by utilising the methodology of Pinkerton [23]. That, using a potential flow calculation, the corresponding values of normal force and incidence were matched by ignoring the Kutta condition. To obtain the critical normal force coefficient, Leishman et al. [2] replaced this method by choosing the static value of C_N that corresponded to either the pitching-moment break or the chord force at stall.

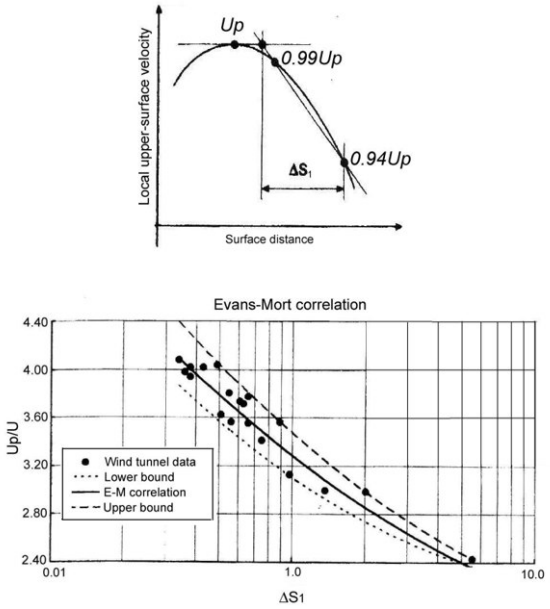

Figure 3 Evans-Mort correlation (as adopted by Niven et al. [22])

Under dynamic conditions, a positive pitch rate decreases the leading edge suction, due to the induced camber effect, so delaying the achievement of the critical normal-force. Hence, for practical purposes, and as an analogue to the static case, Beddoes introduced a time constant T_p to produce an artificial normal-force coefficient, C'_N, that lagged the predicted normal force, but was consistent with the dynamic response of the leading edge pressures. This lagged C'_N did not reach the stall criterion until well after the static-stall angle had been achieved, so reproducing the observed dynamic overshoot of C_N. The lagging was performed by

$$\Delta C'_N(s) = \Delta C_N(s)\left(1 - e^{-s/T_p}\right) \tag{1}$$

where

$$\Delta C_N(s) = C_N(s) - C_N(s - \Delta s)$$

$$\Delta C'_N(s) = C'_N(s) - C'_N(s - \Delta s)$$

Figure 4 depicts the static leading edge C_p against C_N (square symbols). The dashed line is the equivalent dynamic data, whilst the solid line is the lagged value, C'_N. The effect this had on the stall-onset prediction is illustrated in Figure 5.

Here, the Evans-Mort criterion is denoted by C_{N1}. The predicted fully attached-flow triggers the criterion at α_{ss}, as would have been expected and well before the actual dynamic-stall onset at about α_{ds}. The T_p lagged value, α_{tp}, is closer to the observed stall but, for these low-speed data, still some way off; see also Figure 6.

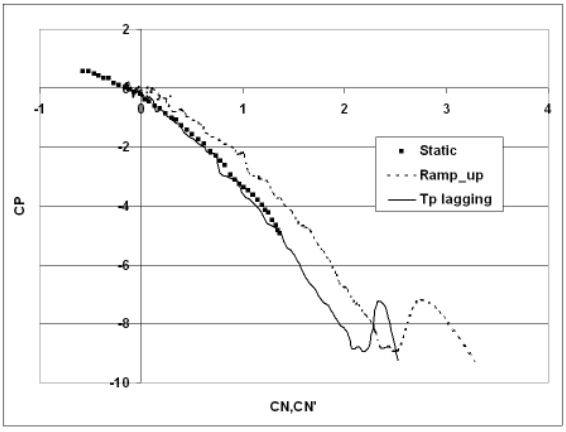

Figure 4 Normal force lagging for a ramp-up test

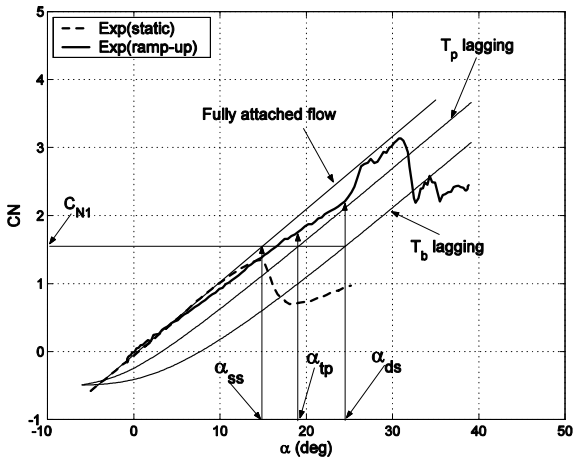

Figure 5 Effects of T_p and T_b lagging

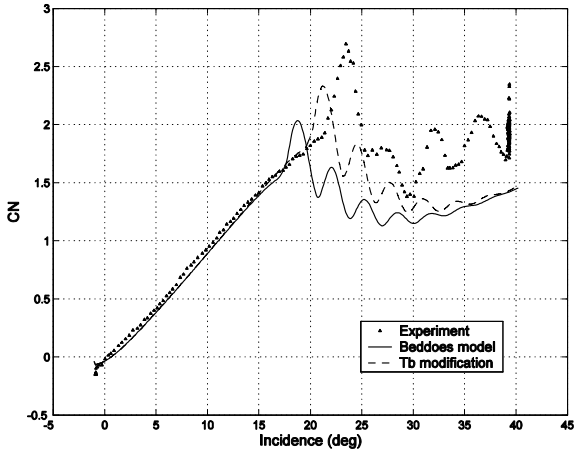

Figure 6 Normal force predictions for ramp-up test (Evans-Mort criterion), r =0.011 (NACA0012)

Parameters: Beddoes model: C_{N1} =1.57 , T_p =1.5

Niven et al's modification: T_b =3.95

Niven et al. [22] had noted this and improved the assessment by simply extending the stall onset by an additional delay function. This required and additional constant, T_b, to extend the lagging by

$$\Delta C_N''(s) = \Delta C_N'(s)\left(1 - e^{-s/T_b}\right) \tag{2}$$

and this yielded predictions that were much closer to the observed stall onset (as may be seen in Figures 5 & 6).

The agreement, however, was not as good for all aerofoils and the uncertainties associated with the Evans-Mort upper and lower limits render the assessments of T_b somewhat subjective.

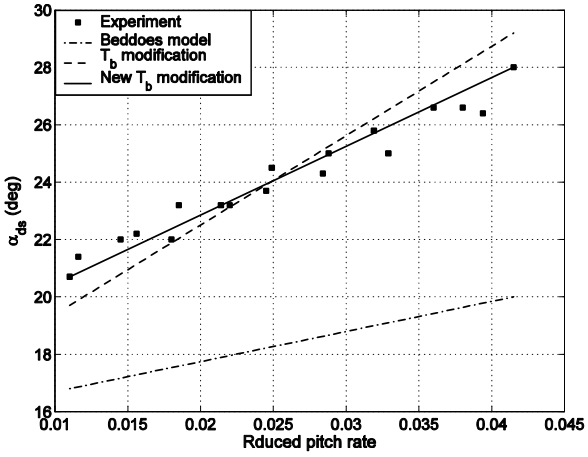

Figure 7 Comparison of Mort-Evans criterion

Beddoes model: $C_{N1} = 1.57$, T_p =1.5

Niven et al's modification: T_b=3.95

New modification: $C_{N1} = 1.75$, T_p =1.5, T_b=2.2

Figure 7, illustrates the test data for the onset of dynamic-stall and the predictions using T_p (dash-dotted line) and with T_b modification (broken line) for NACA0012. It can be seen that T_b modification gives much closer agreement with the experimental data.

From Figure 7, however, it can be seen that, based on the Evans-Mort criterion, the T_b modification under-predicts stall onset for lower reduced pitch rates, and over-predicts onset for higher values. This can be rectified by a judicial selection of C_{N1} and T_b. For example, if C_{N1} increases from 1.57 (Evans-Mort criterion) to 1.75, and T_b decreases from 3.93 to 2.2, the improved result is as shown in Figure 7 (solid line), compared to Niven's modification (broken line).

In the Niven et.al. paper [22], the NACA 23012B aerofoil (with the Beddoes value of T_p applied, and using an upper bound of Evans & Mort) did not give a consistent agreement with the model (dashed line Figure 8). When, however, a lower bound of Evans and Mort was adopted (dotted line in Figure 8), then including the T_b modification (solid line) gave a good prediction.

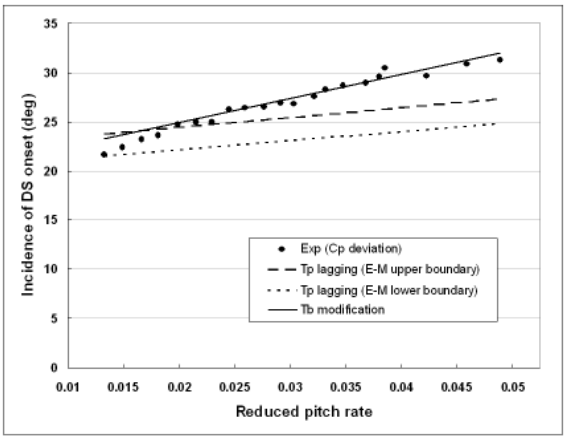

Figure 8 Dynamic stall onset for NACA23012B aerofoil

(reproduced from Niven et.al [22])

The above tends to indicate the problematic nature of the current low-speed criterion for dynamic stall onset in as much as it requires the selection of C_{N1} value within the upper and lower bounds of the Evans and Mort correlation, a value for T_p and a further value for T_b. Hence, for each aerofoil, three interdependent constants must be specified. It is this inherent subjectivity and the variability within the Evans-Mort correlation that provided the incentive for the present work to seek a new and consistent stall onset criterion.

2 Definitions of dynamic-stall onset

Due to the complexity of the dynamic-stall process, several researchers have explored incipient stall by applying a range of techniques to measured data. Some of these involved the examination of air loads [1,8,24,25], while others, the examination of flow field data of pressure [26,27] and smoke-flow visualization [28].

A selection of stall onset assessments is presented in Figure 9. They include, C_N deviation (as illustrated in Figure 1 and 9a), The pitching moment break defined as a 0.05 drop in C_m (9b), The drag coefficient deviation (9c), the maximum value

of chord force coefficient C_c (9d), the C_p deviation at about quarter-chord (9e) and the suction collapse of pressure at the leading edge (9f).

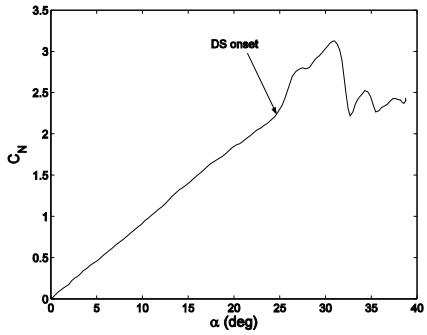

(a) C_N deviation

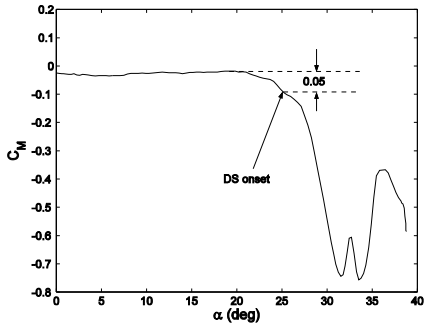

(b) C_m break ($\Delta C_m = 0.05$)

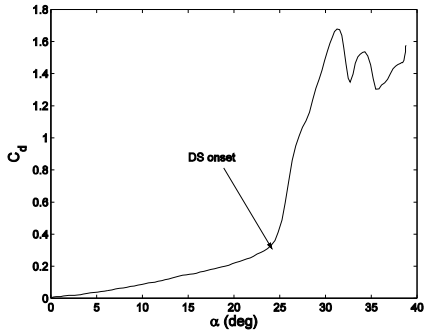

(c) C_d deviation

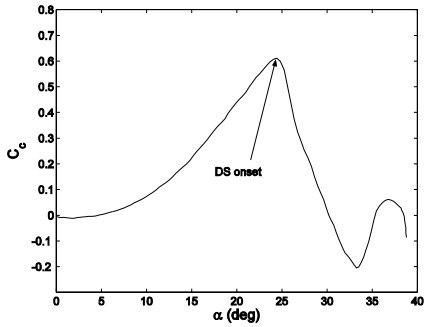

(d) C_c maximum

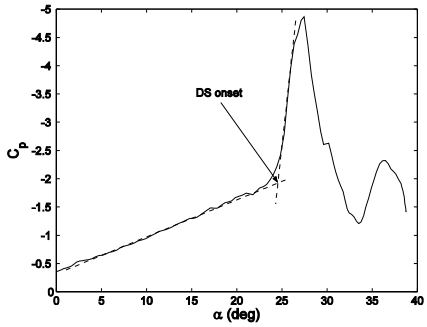

(e) C_p deviation

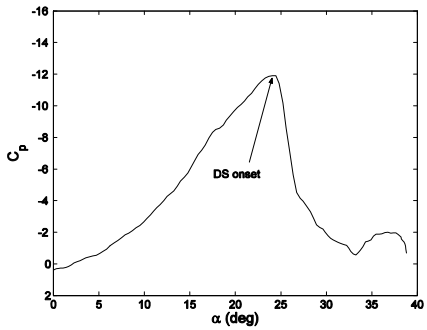

(f) C_p collapse at LE

Figure 9 Definitions of dynamic stall-onset

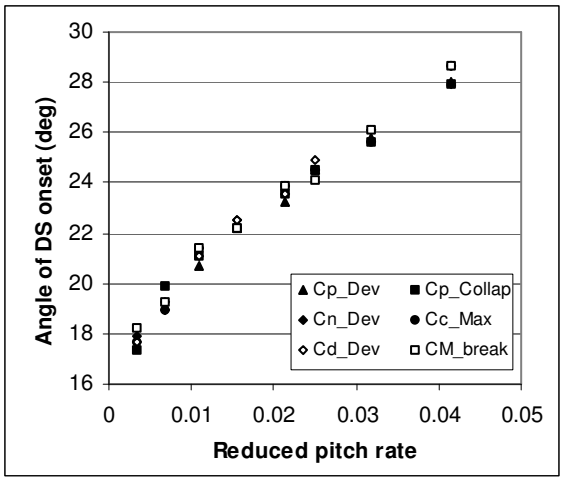

Figure 10 Onset of dynamic stall by different definitions (NACA 0012)

All the above methods are compared in Figure 10 where it may be seen that, in general, they all yield similar and acceptable results. As such, for the purposes of predicting the overall aerodynamic coefficients, any of these definitions could be acceptable. On the basis that, the C_c maximum criterion yields easily obtainable and relatively unambiguous result; it has been used throughout this paper. This has the advantage that local disturbances do not significantly affect the integrated general result.

3 A new model for predicting dynamic stall onset

The present authors have revisited the unsteady data gathered from 13 aerofoils at the University of Glasgow in their low-speed Handley-Page wind tunnel facility. The aerofoils that have been tested are listed in Table 1 (Galbraith et al 1992a [29]).

For the study of dynamic stall on helicopter rotor blades, a family of aerofoils derived from the NACA23012 section were tested. The family includes 12%-thick NACA23012A and NACA23012C sections, which are identical to the NACA23012 over the leading 25% chord, but modified to produce a reflex trailing-edge and increased positive camber respectively. The NACA23012B, is a 16%-thick aerofoil derived from the NACA23012 and an RAE section. During work considering the aerodynamics of vertical-axis wind turbines (VAWT's), six NACA 4-digit symmetrical aerofoils were considered. These were a NACA0012, NACA0015, NACA0018, NACA0021, NACA0025 and NACA0030. Additionally, a NACA 0015 aerofoil with a chord length of 0.275m and an AR of 5.85, instead of the usual 0.55m chord and AR of 2.93, was tested to assess the effects of aspect ratio during tunnel tests.

During the work on the dynamic stalling of wind turbine rotors, further tests were performed on a 21%-thick symmetrical AHAVAW aerofoil and a NACA0018 with a modified leading edge (the GUVA10 section). The profiles for all of these aerofoils are illustrated in Figure 11.

All ramp up data from the above aerofoils have been analysed to obtain the angle at which the stall occurs. The results, for six aerofoils, are presented as the black squares in Figure 12. It may be noticed that, above a reduced pitch rate of 0.01, the data increase linearly with reduced pitch rate. According to Seto and Galbraith [26], a reduced pitch rate of 0.01 delimits the boundary of quasi-static and dynamic stall. At low reduced pitch rate, the pressure profile characteristics are qualitatively similar to those in steady conditions, but with some lift and moment overshoot (quasi-static stall). At higher reduced pitch rates, as depicted in Figure 1, the stall is markedly different from the static case and is termed deep dynamic-stall. Similarly, Beddoes [44] noted that criticality of the leading edge, for the initiation of dynamic stall, only occurred when the pitch rate exceeded some small positive value.

Model No.	Aerofoil Section	Thickness	Chord Length	Span	Pitch Axis	Reference No.
1	NACA23012	12%	0.55m	1.61m	0.25c	30,31
2	NACA23012A	12%	0.55m	1.61m	0.25c	32
3	NACA23012B	16%	0.55m	1.61m	0.25c	33
4	NACA23012C	12%	0.55m	1.61m	0.25c	34
5	NACA0015	15%	0.55m	1.61m	0.25c	35
6	NACA0018	18%	0.55m	1.61m	0.25c	36
7	NACA0021	21%	0.55m	1.61m	0.25c	36
8	NACA0025	25%	0.55m	1.61m	0.25c	38
9	NACA0030	30%	0.55m	1.61m	0.25c	39
10	NACA0012	12%	0.55m	1.61m	0.25c	40
11	NACA0015	15%	0.275m	1.61m	0.25c	41
12	AHAVAW	21%	0.55m	1.61m	0.25c	42
13	GUVA10	18%	0.55m	1.61m	0.25c	43

Table 1 List of aerofoils tested at Glasgow University

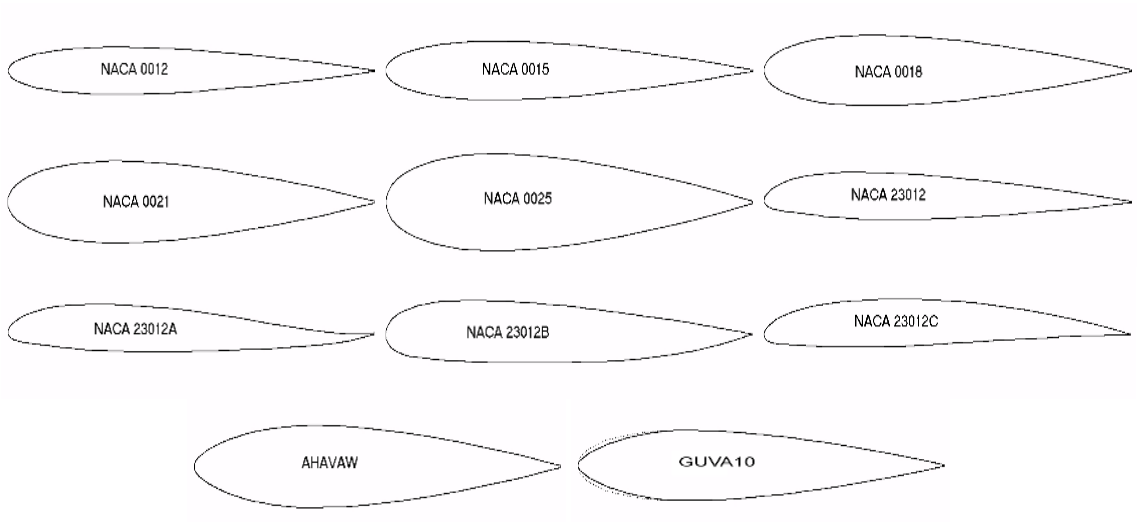

Figure 11 Profiles of aerofoils tested (in GUVA10 the dot line is the profile of NACA0018)

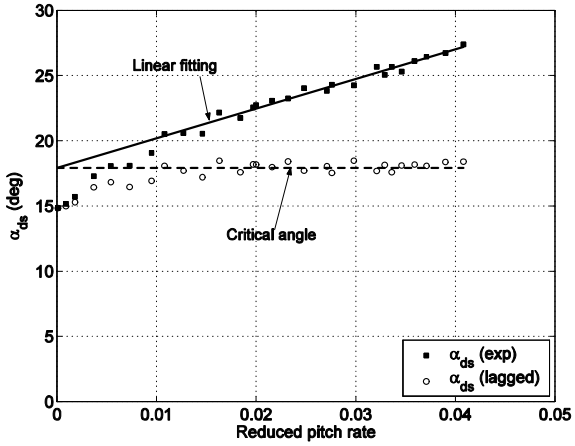

(a) NACA 23012

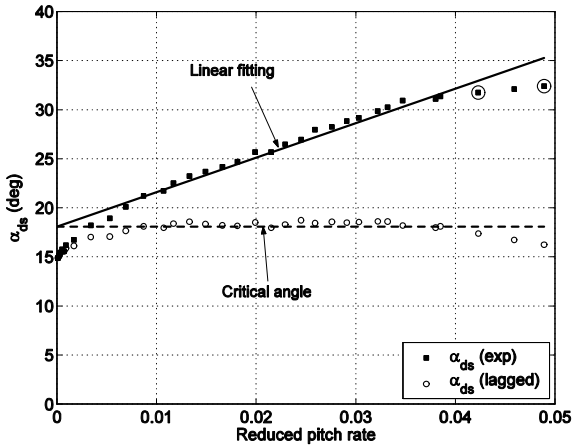

(b) NACA 23012B

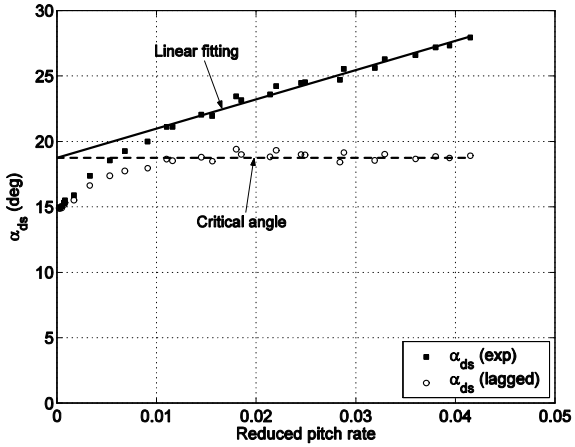

(c) NACA 0012

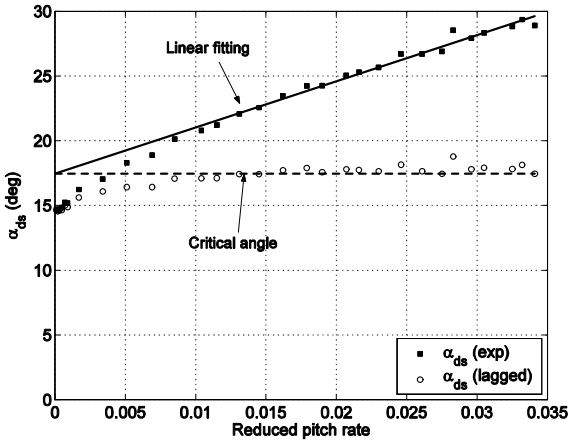

(d) NACA 0018

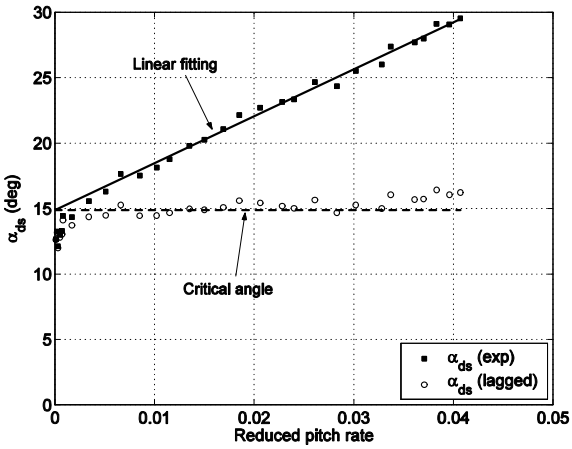

(e) AHAVAW

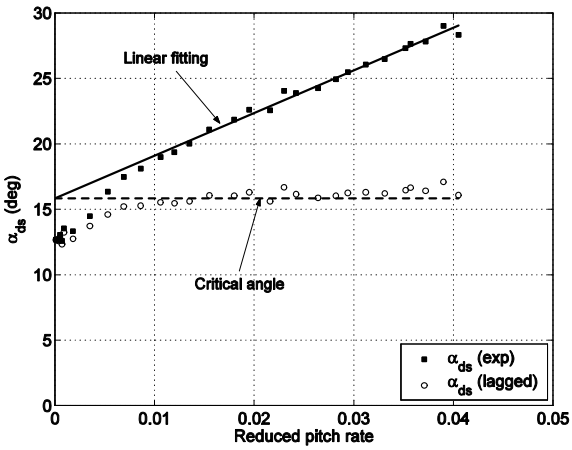

(f) GUVA10

Figure 12 Incidences of dynamic stall-onset

Given the appearance of the stall onset data, and as shown by Wilby [45], beyond a certain reduced pitch rate, a linear relationship exists between the onset angles of dynamic stall and reduced pitch rates. A suitable linear fitting form is given by:

$$\alpha_{ds} = D_1 r + \alpha_{ds0} \tag{3}$$

where α_{ds0} is obtained via a backward extrapolation of the trend line from r = 0.01 to 0.0.

As may be seen, the fit (solid lines in Figure 12) works well. It should be noted, however, that, for a NACA 23012B, when the reduced pitch rate is greater than 0.04, the onset data deviate from the trend line. This is primarily due to a limitation of the test set-up, since the normal maximum angle of attack is 35°. Towards the end of the pitch up, the motion, necessarily, becomes non linear as the rotation slows down (discussed further in Section 4). None of the other stall data exceed 30°.

A dimensionless time constant, T_α may now be defined as:

$$T_\alpha = \frac{\alpha_{ds} - \alpha_{ds0}}{\dot{\alpha}} \frac{2V_\infty}{c} = \frac{\alpha_{ds} - \alpha_{ds0}}{r} \frac{\pi}{180} = \frac{\pi}{180} D_1 \tag{4}$$

For ramp data, this effectively defines the time taken from reaching α_{ds0} to stall onset. Table 2 lists the numerical values obtained for both α_{ds0} and the associated time delay T_α.

It is interesting to note that for all the NACA series aerofoils, all the values of α_{ds0} are similar, regardless of the aerofoil thickness and camber, except for the last two aerofoils (AHAVAW and GUVA10) which were designed to stall early.

Aerofoil	α_{ds0} (deg)	T_α
NACA0012	18.73	3.90
NACA0015 (chord=0.55m)	17.81	5.78
NACA0015 (chord=0.275m)	16.79	5.94
NACA0018	17.46	6.22
NACA0021	17.91	6.30
NACA0025	17.22	6.95
NACA23012	17.91	3.97
NACA23012A	17.19	5.11
NACA23012B	18.07	6.14
NACA23012C	18.06	5.59
AHAVAW*	14.88	6.27
GUVA10*	15.82	5.70

Table 2 α_{ds0} and T_α for NACA aerofoils

When an angle lagging, in the form,

$$\Delta\alpha'(s) = \Delta\alpha(s)\left[1 - e^{-s/T_\alpha}\right] \tag{5}$$

is applied, the lagged stall-onset angles (identified by small circles in Figure 12) are close to the critical angle, α_{ds0} .

The above may now be re-stated as a criterion for dynamic-stall onset:

- The angle, α_{ds0} , and the dimensionless time constant T_α for each aerofoil, are obtained from series ramp-up tests using Equations (3 & 4)
- Lagged incidence α' is obtained via Equation (5)
- Stall onset occurs when $\alpha' > \alpha_{ds0}$.

This new low-speed stall criterion appears to be more deterministic than the C_N lagged criterion of Beddoes [2,3], including the Niven et. al. [22] modification of a further T_b lagging. The basic difference between these two criteria is illustrated in Figure 13, where the values of C_N lagging and α lagging trigger the stall when the respective criticalities are reached.

In the following section, the general applicability of the new model is studied by considering a range of pitching motions in addition to basic ramp up motions.

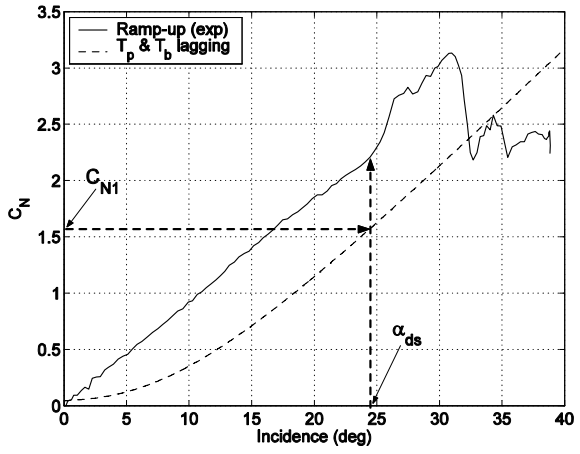

(a) Evans-Mort correlation with T_p and T_b lagging

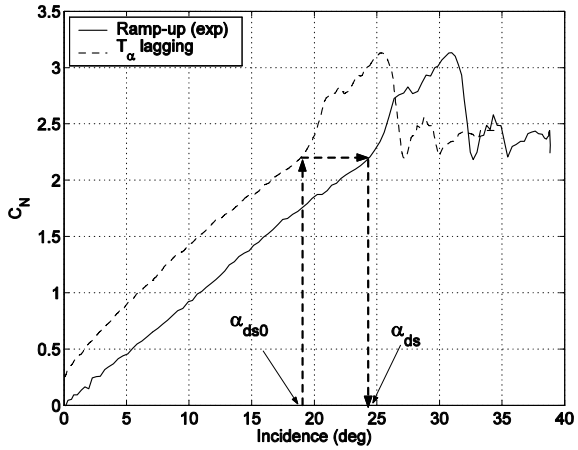

(b) New stall criterion (this paper)

Figure 13 Comparison of the two criteria

4 Results and Analysis

Figure 14 illustrates the agreement the new criterion provides when adopted into the Beddoes/Leishman model [2,3]. The agreement is, as to be expected, very good in as much as it was from these data that the criterion was developed. It should be remembered, however, that the purpose of the Beddoes-Leishman model was to, based on first order physics and flow phenomena descriptors, re-construct the unsteady aerodynamic coefficients. On that basis, it is far more sophisticated than a simple curve fitting routine. The agreement for all the ramp-up data illustrates the quality of this new stall criterion, albeit for tests carried out in a single tunnel.

It may be expected, from Figure 14, the predictions for ramp-up aerofoil performance will be well predicted; Figure 15 confirms this. Included in that figure are the third generation formulations where the effects of T_p and T_b by way of comparison.

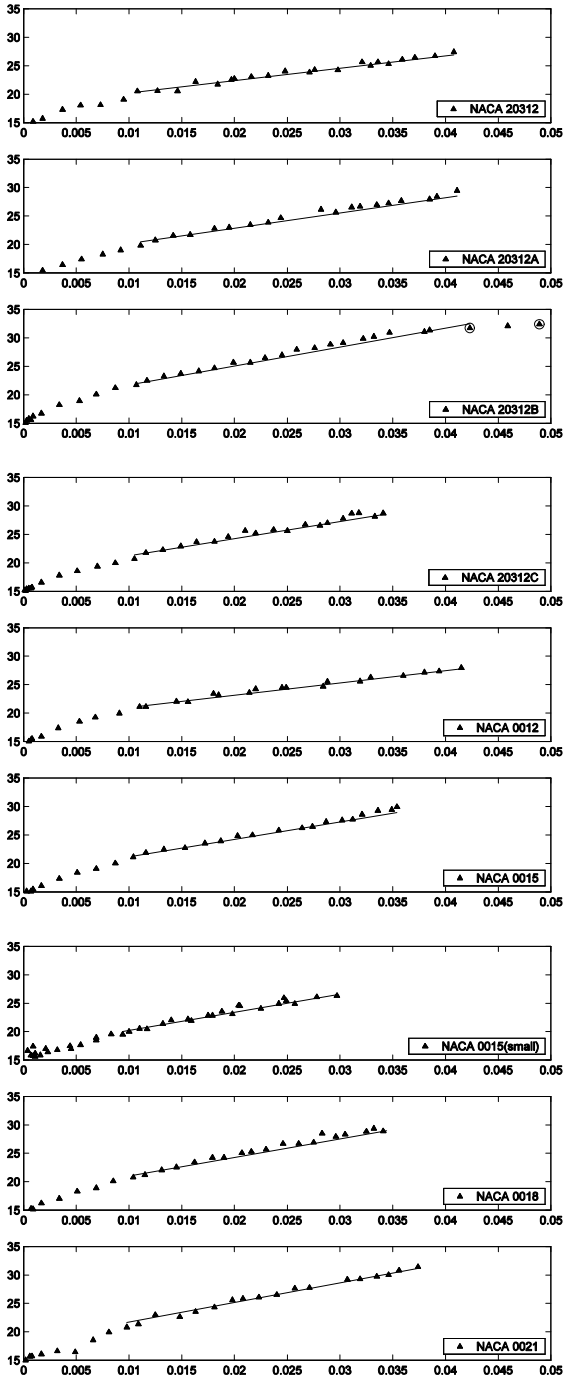
NACA 20312
NACA 20312A
NACA 20312B
NACA 20312C
NACA 0012
NACA 0015
NACA 0015(small)
NACA 0018
NACA 0021

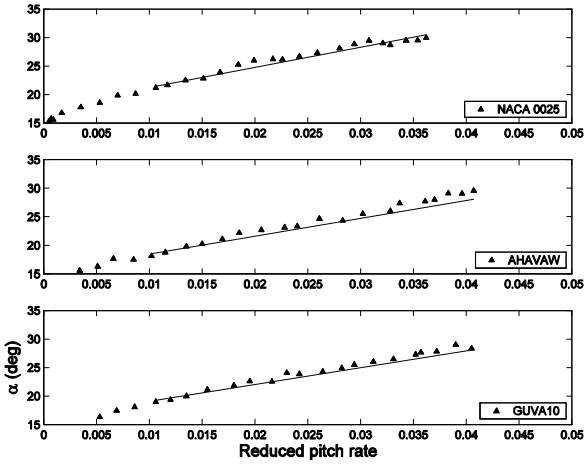

Figure 14 Predictions of dynamic-stall onset (solid line), compared to Glasgow data (black triangles)

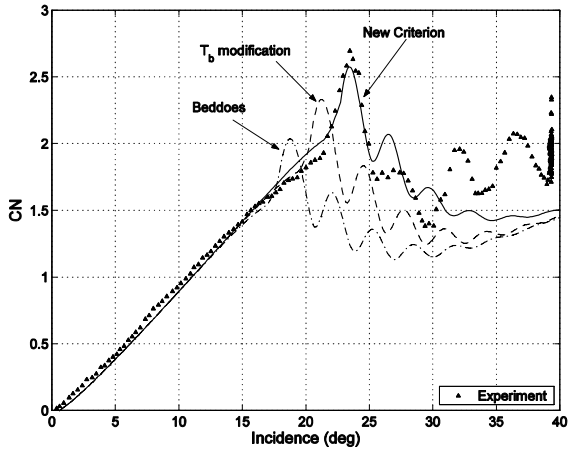

Figure 15 Reconstructions of normal force for a ramp-up test of r =0.011 (NACA0012)

Parameters: Beddoes model: C_{N1}=1.57, T_p=1.5

Niven et al modification: T_b=3.93

Present criterion: α_{ds0} = 18.73^0, T_α=3.90

Once again noting, that the above predictions are re-constructions of the data from whence they came, it is important that the new criterion can faithfully predict the onset of stall for all pitching motions and in particular, oscillatory motions. Figures 16-17 clearly illustrate the improved and consistent predictions of such data.

The above results confirm that the new criterion derived from ramp-up data, is also applicable to oscillatory and, possibly any pitching motion.

This last comment is particularly relevant to the NACA 23012B aerofoil in which, it may be recalled from Section 3, that the trend line over predicted the measured data for a reduced pitch rate greater than 0.04. This, it was suggested, was a consequence of the actual test ramp-up reaching the non-linear deceleration phase. To emphasise this and confirm the cause, Figures 18 and 19 show the predictions for the NACA 23012B aerofoil having undergone ramp-up tests, of reduced pitch rate 0.0423 and 0.0489, using the measured pitch profile of the experiment to drive the calculation. It may be seen that the stall onset occurs in the non-linear zone and is predicted well when compared to the prediction of ideal ramp-ups (dashed lines).

Further confirmation has been included in Figure 12b where the large circles indicate the above triggering of the new stall criterion for these two cases. The reasons given (Section 3) for the trend line overshoot are therefore validated.

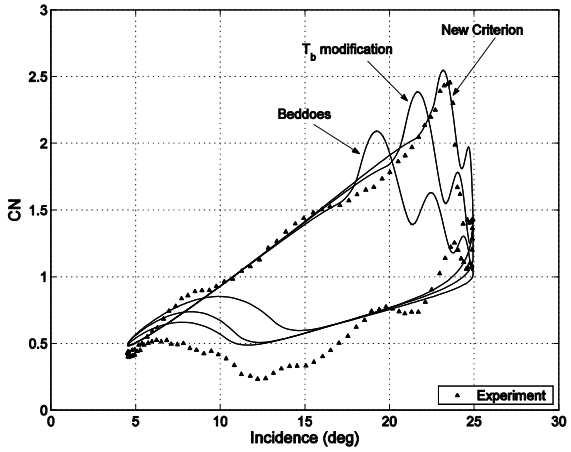

Figure 16 Reconstructions of normal force for an oscillating test for NACA0012 ($\alpha = 15^0 + 10^0 \sin \omega t$, $\kappa = 0.075$)

Parameters: same as in Figure 15

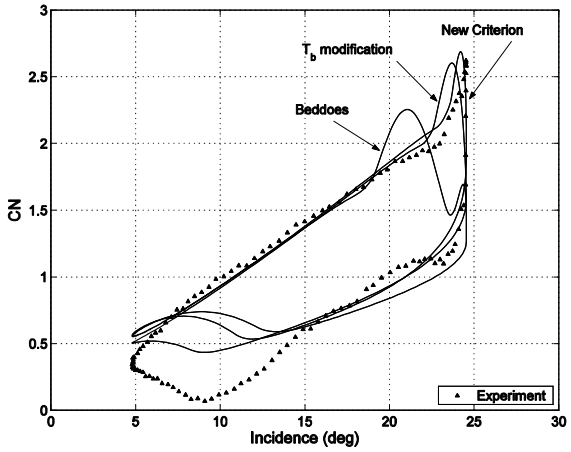

Figure 17 Reconstructions of normal force for an oscillating test for NACA0012 ($\alpha = 15^0 + 10^0 \sin \omega t$, $\kappa = 0.124$)

Parameters: same as in Figure 15

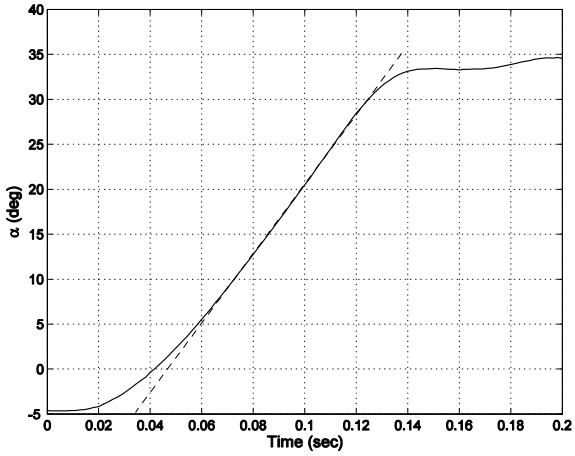

(a) Time history of incidence

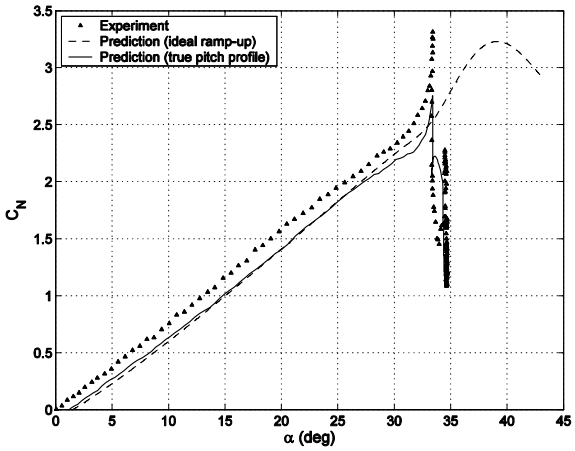

(b) Ramp-up normal force prediction

Figure 18 NACA23012B high ramp rate prediction (r =0.0423)

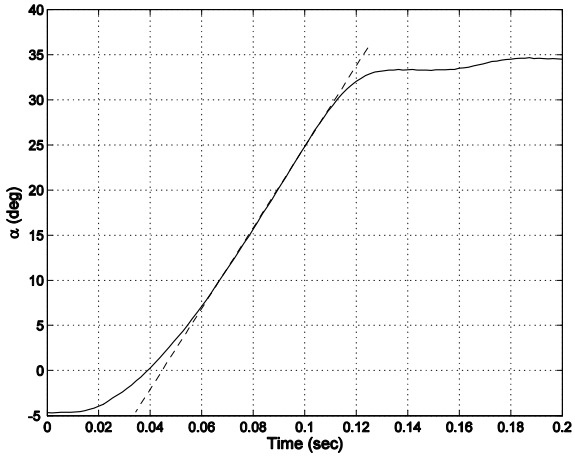

(a) Time history of incidence

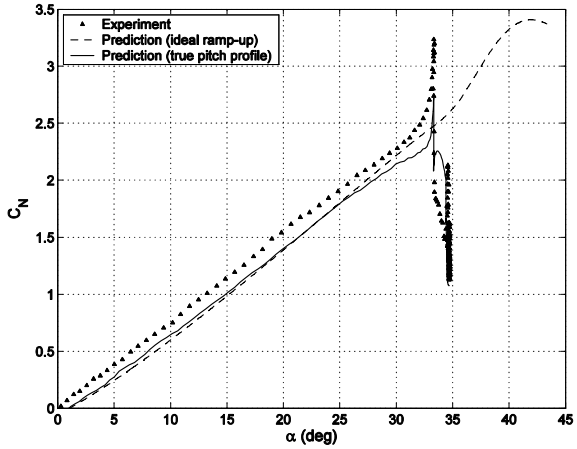

(b) Ramp-up normal force prediction

Figure 19 NACA23012B high ramp rate prediction (r =0.0489)

5 Conclusions

For low-speed dynamic stall of pitching aerofoils, a new stall-onset criterion has been developed with significant improvements over the original criterion of Beddoes [2,3] and the modified version of Niven et.al [22]. In particular the following has been demonstrated for low-speed dynamic stall;

1) Stall onset is well represented by the incidence at the maximum chord force coefficient.

2) For ramp-up data, beyond a certain reduced pitch rate (r>0.01), the dynamic-stall onset varies linearly with reduced pitch rate.

3) Extrapolating the stall data backwards to a reduced pitch rate of zero gives an incidence value, unique to each aerofoil, of α_{ds0}.

4) From α_{ds0} an associated time delay T_α was obtained.

5) A lagged incidence α', when compared to the actual incidence, was obtained in the form;

$$\Delta\alpha'(s) = \Delta\alpha(s)\left[1 - e^{-s/T_\alpha}\right]$$

6) Dynamic stall occurs when $\alpha' > \alpha_{ds0}$.

7) It was shown that the new formulation yielded improved predictions over the previous criterion.

8) The new criterion is probably applicable to all pitching motions associated with dynamic stall, and in particular oscillatory, pure ramp and distorted ramp functions as in Figure 18 and 19.

Acknowledgements

This research work is sponsored by British Engineering and Physics Science Research Council (EPSRC), Research Grant No.GR/S42446/01, in collaboration with Garrad Hassan Ltd. and the National Renewable Energy Laboratory's, National Wind Turbine Centre, Colorado, USA

Nomenclature

V =Free stream velocity

C_N =Normal force coefficient

C_m =Pitching moment coefficient

C_d =Drag coefficient

C_p =Pressure coefficient

C_c =Chordwise force coefficient

T_α =Time delay constant for angle of attack

T_p =Time delay constant for normal force.

T_b =Time delay constant for Niven's modification

s =Non-dimensional time ($s = \frac{2Vt}{c}$)

κ =Reduced frequency ($\kappa = \frac{\omega c}{2V}$)

r =Reduced pitch rate ($r = \frac{\dot{\alpha} c}{2V}$)

α =Angle of attack or incidence

α_{ss} =Angle of static stall

α_{ds} =Angle of dynamic stall onset

α_{ds0} =Critical angle for dynamic stall onset

C_{N1} =Evans-Mort critical value of normal force

ΔS_1 =Approximate distance between peak velocity and laminar separation point (%chord)

LE =Leading-edge

M =Mach number

DS =Dynamic stall

CFD =Computational Fluid Dynamics

References

[1] Beddoes T. S., 1976, "A Synthesis of Unsteady Aerodynamic Effects Including Stall Hysteresis", *Vertical 1*: 113-123

[2] Leishman J.G, Beddoes T.S., 1989, "A Semi-Empirical Model for Dynamic Stall", *Journal of the American Helicopter Society* 34: 3-17

[3] Beddoes T.S., 1993, "A Third Generation Model for Unsteady Aerodynamics and Dynamic Stall", Westland Helicopter Limited, RP-908

[4] Carr L.W., 1988, "Progress in Analysis and Prediction of Dynamic Stall", *Journal of Aircraft* 25: 6-17

[5] Niven A.J, Galbraith R.A.McD, Herring D.G.F, "Analysis of Reattachment during Ramp Down Tests", *Vertica* 13: 187-196, 1989

[6] Carr L.W, Chandrasekhara M.S, 1996, "Compressibility Effects on Dynamic Stall", *Progress in Aerospace Science 32*: 523-573

[7] Leishman J.G., 2000, *Principles of Helicopter Aerodynamics*, Cambridge University Press

[8] Wilby P.G., 1980, "The Aerodynamic Characteristics of Some New RAE Blade Sections, and Their Potential Influence on Rotor Performance", *Vertica 4:* 121-133

[9] Gross D.W, Harris F.D., 1969, "Prediction of In-Flight Stalled Airloads from Oscillating Airfoil Data", 25th Annual Forum of the AHS, Washington DC

[10] Johnson W., 1969, "The Effect of Dynamic Stall on the Response and Airloading of Helicopter Rotor Blades", *Journal of American Helicopter Society 14*:68-77

[11] Carta F.O. et al., 1970, "Analytical Study of Helicopter Rotor Stall Flutter", 26th Annual Forum of the AHS, Washington DC

[12] Tran C.T, Petot D., 1981, "Semi-Empirical Model for the Dynamic Stall of Airloads in View of the Application to the Calculation of Responses of a Helicopter Blade in Forward Flight", *Vertica 5*:35-53

[13] Gangwani S.T., 1984, "Synthesized Airfoil Data method for Prediction of Dynamic Stall and Unsteady Airloads", *Vertica 8*:93-118

[14] Jones K.D, Platzer M.F., 1998, "On the Prediction of Dynamic Stall Onset on Airfoils in Low Speed Flow", Proceedings of the 8th International Symposium on Unsteady Aerodynamics and Aeroelasticity of Turbomachines, Dordrecht, the Netherlands

[15] Ekaterinaris J.A, Platzer M. F., 1997, "Computational Prediction of Airfoil Dynamic Stall", *Progress in Aerospace Science* 33: 759-846

[16] Beddoes T.S., 1983, "Representation of Airfoil Behaviour", *Vertica* 7: 183-197

[17] Beddoes T.S., 1984, "Practical Computational of Unsteady Lift", *Vertica* 8: 55-71

[18] Leishman J.G., 1987a, "Practical Modelling of Unsteady Airfoil Behaviour in Nominally Attached Two-Dimensional Compressible Flow", UM-AERO-87-6, Department of Aerospace Engineering, University of Maryland

[19] Leishman J.G., 1987b, "A Semi-Empirical Model for Dynamic Stall", UM-AERO-87-24, Department of Aerospace Engineering, University of Maryland

[20] Beddoes T.S., 1983, "Representation of Airfoil Behaviour", *Vertical 7*: 183-197

[21] Evans W.T, Mort K.W., 1959, "Analysis of Computed Flow Parameters for a Set of Suddenly Stalls in Low Speed Two-Dimensional Flow", NACA TND-85

[22] Niven A.J, Galbraith R.A.McD., 1997, "Modelling Dynamic Stall Vortex Inception at Low Mach Numbers", *The Aeronautical Journal 101:*67-76

[23] Pinkerton R.M., 1936, "Calculated and Measured Pressure Distributions over the Midspan Section of the NACA4412 Aerofoil", NACA Report 563

[24] Scruggs R.M, Nash J.F, Singleton R.E., 1974, "Analysis of Dynamic Stall Using Unsteady Boundary Layer Theory", NASA CR-2462

[25] Wilby P.G., 1984, "An Experimental Investigation of the Influence of a Range of Aerofoil Design Features on Dynamic Stall Onset", presented at 10th European Rotorcraft Forum

[26] Seto L.Y, Galbraith R.A.McD., 1985, "The Effect of Pitch-Rate on the Dynamic Stall of a NACA23012 Aerofoil", 11th European Rotorcraft Forum, London

[27] Lorber P.F, Carta F.O., 1987, "Airfoial Dynamic Stall at Constant Pitch Rate and High Reynolds Number", presented at AIAA 19th Fluid Dynamics, Plasma Dynamics and Lasers Conference, AIAA 87-1329

[28] Daley D.C., 1984, Jumper E.J, "Experimental Investigation of Dynamic Stall for a Pitching Airfoil", *Journal of Aircraft*, Vol. 21

[29] Galbraith R.A.McD, Gracey M.W, Leitch E., 1992b, "Summary of Pressure Data for Thirteen Aerofoils on the University of Glasgow's Aerofoils Database", GU Aero Report 9221

[30] Seto L.Y, Galbraith R.A.McD., 1984, "The Collected Data for Ramp Function Tests on a NACA23012 Aerofoil", Vol.1, GU Aero Report 8413

[31] Leishman J.G, Seto L.Y, Galbraith R.A.McD., 1984, "Collected Data for Oscillatory Pitch Tests on a NACA23012 Aerofoil", Vol. 1&2, GU Aero Report 8404

[32] Niven A.J, Gracey M.W, Galbraith R.A.McD., 1992, "Collected Data for Tests on a NACA23012A Aerofoil", GU Aero Report 9220

[33] Herring D.G.F, Galbraith R.A.McD., 1988, "The Cellected Data for Tests on a NACA23012B Aerofoil", Vol. 1-4, GU Aero Report 8809-8811

[34] Gracey M.W, Galbraith R.A.McD., 1989, "Collected Data for Tests on a NACA23012C Aerofoil", Vol.1&2, GU Aero Report 8901

[35] Angell R.K, Musgrove P.J, Galbraith R.A.McD., 1988a, "Collected Data for Tests on a NACA0015", Vol. I-III, GU Aero Report 8803

[36] Angell R.K, Musgrove P.J, Galbraith R.A.McD., 1988b, Collected Data for Tests on a NACA0018, Vol. I-III, GU Aero Report 8815

[37] Angell R.K, Musgrove P.J, Galbraith R.A.McD, 1988c, Collected Data for Tests on a NACA0021, Vol. I-III, GU Aero Report 8802

[38] Angell R.K, Musgrove P.J, Galbraith R.A.McD., 1988d, "Collected Data for Tests on a NACA0025", Vol. I-III, GU Aero Report 8822-8824

[39] Angell R.K, Musgrove P.J, Galbraith R.A.McD., 1988e, "Collected Data for Tests on a NACA0030", Vol. I-III, GU Aero Report 8825-8827

[40] Galbraith R.A.McD, Gracey M.W, Gilmour R., 1992b, Collected Data for Tests on a NACA0012 Aerofoil, Vol. I-II, GU Aero Report 9207-9208

[41] Galbraith R.A.McD, Jiang Dachun, Green R.B, Gracey M.W, Gilmour R., 1992c, "Collected Data for Tests on a NACA0015 Aerofoil with Chord of Length 0.275m", GU Aero Report 9209

[42] Jiang Dachun, Galbraith R.A.McD, Coton F.N, Gracey M.W, Gilmour R., 1992a, "Collected Data for Tests on an AHAVAW Aerofoil", Vol. I-III, GU Aero Report 9212-9214

[43] Jiang Dachun, Galbraith R.A.McD, Gracey M.W, Gilmour R., 1992b, "Collected Data for Tests on a GUVA10 Aerofoil", Vol. I-III, GU Aero Report 9217-9219

[44] Beddoes T.S., 1978, "Onset of Leading Edge Separation Effects under Dynamic Conditions and Low Mach Number", presented at the 34th Annual National Forum of the American Helicopter Society, Washington D.C

[45] Wilby P.G., 2001, "The Development of Airfoil Testing in the UK", *Journal of American Helicopter Society* 46: 210-220

List of Figures

List of Tables